APPLICATION OF 0-1 TEST FOR CHAOS IN WIND TUNNEL AEROELASTIC EXPERIMENTS OF AN ALUMINUM FLAT PLATE

Michelle F. Westin[1], Roberto G. A. da Silva[1], and José M. Balthazar[2]

[1] Technological Institute of Aeronautics
São José dos Campos, São Paulo, Brazil
mifwestin@gmail.com
gil@ita.br

[2] Federal Technological University of Paraná
Ponta Grossa, Paraná, Brazil
jmbaltha@gmail.com

Keywords: 0-1 test, chaos, nonlinear aeroelasticity, wind tunnel, flutter.

Abstract: Nonlinear aeroelastic phenomena are continuously investigated in aeronautical researches. The nonlinearity nature can be aerodynamic or structural. This work will investigate aeroelastic nonlinearities in a very flexible wing. A flutter analysis is proceeded in order to evaluate the error between the computational results and the experiment. Since the linear flutter theory considers small disturbances, nonlinear phenomena are expected. Both wind tunnel and computational experiments time series shall be analyzed and the evaluation if the system presents chaotic behavior will be performed through the 0-1 test.

1 INTRODUCTION

The physical phenomenon that will be investigated in this work is flutter and the consequently nonlinearity due to the wing high flexibility. The present investigation scope is the experimental aeroelastic analysis of flexible wings using subsonic wind tunnels.

To achieve this objective, it is necessary to design wings in which the flutter velocity is below the wind tunnel speed range. Also, it is important to study a methodology to identify the moment when flutter onsets during the test despite its nonlinearity. The flexible wings design is very important to provide models that can be used in further researches for smart materials applications, for example.

The phenomena under experimental investigation unifies high aspect ratio wings design for wind tunnel flutter tests [1], and a procedure used by Sheta, Harrand, Thompson and Strganac [2] to identify the flutter onset power spectral density versus frequency. After the wind tunnel flutter test, it was verified that the aeroelastic system tested presented nonlinear behavior that might be limit-cycle oscillations (LCO) [3]. So, computational experiments were conducted using a nonlinear aeroelastic tool called Aero Flex [4] and the same aeroelastic system. This tool is more suitable for nonlinear aeroelasticity analysis, mainly for geometric or structural nonlinearities which shall be the main source of nonlinearities for high aspect ratio wings.

The main objective is to demonstrate the application of the 0-1 test for chaos [5] in an aeroelastic system. The verification if a nonlinear aeroelastic system is chaotic or if it is an LCO is very important, since chaos is not desirable in any structure. This test only requires a time history,

so it can be applied for both wind tunnel experiments and computational experiments. The 0-1 test is based on statistical properties of a variable and the main advantage is that the attractor reconstruction is no longer necessary, at least for a qualitative analysis.

The system dynamics reconstruction applies the Takens' theory [6], which requires the determination of the embedded dimension [7] and the delay parameter [8]. A poor choice of these parameters leads to a wrong attractor. In this case, determining a wrong attractor means consider as a limit-cycle oscillation that should be chaos instead, and vice-versa.

In this work, the 0-1 test results shall be presented for both aeroelastic wind tunnel test [9] and computational test using AeroFlex. 0-1 test is named after the two possible results of this test: 1 for chaos or 0 for LCO.

This work is organized in the following sections: this brief introduction to the study, the theoretical background in section 2, the linear flutter prediction in section 3, the nonlinear computational results in section 4, the experimental results in section 5, the 0-1 test for chaos for both experimental and computational time histories in section 6 and the conclusion and future researches in section 7.

2 THEORETICAL BACKGROUND

2.1 Linear Aeroelastic System

Flutter is an aerodynamic auto-excited phenomenon which occurs due to the coupling of two or more different vibration modes. This coupling results from the interaction between aerodynamic, elastic and inertial forces. Since flutter is a catastrophic phenomenon, it must be avoided for the entire aircraft flight envelope [10].

For some special cases, such as a wing carrying storages or very flexible wings with high aspect ratio that leads to high displacements, the flutter is not catastrophic. For example, after achieving the flutter velocity, a missile pylon starts to oscillate with a sustainable amplitude. Even when the velocity is increased, the amplitude is the same. This is a classic example of limit-cycle oscillation (LCO), which is a nonlinear phenomenon. If the system presents aperiodic behavior, with high sensitivity to initial conditions, the system present chaotic behavior, as will be presented later.

The flutter prediction methodology is based on the g-method, developed and implemented by ZONA® Technologies, in the software ZAERO®. The wings structural dynamic models are computed using the finite element method implements in NASTRAN® solver (solution 103). Subsequently, ZAERO® software is employed to compute the flutter mechanism. Unsteady aerodynamic loading is computed through a lifting surface interference method known as ZONA 6.

The g method introduces a first order damping perturbation in the flutter equation. So, the equation of motion used to determine flutter velocity is given by [3]:

$$\left[\left(\frac{V}{L}\right)^2 Mp^2 + \left(\frac{V}{L}\right) Bp + K\right]\{\xi(p)\} = q[Q(ik) + gQ'(ik)]\{\xi(p)\} \quad (1)$$

where, *V* is the undisturbed flow velocity, *L* is a reference length, *M* is the generalized mass matrix, *B* is the generalized damping matrix, *K* is the generalized stiffness matrix, *ξ(p)* is an eigenvector with the generalized coordinates, *Q(p)* is the generalized aerodynamic force matrix and its derivative related to *k* (reduced frequency) and *p* is defined as:

$$p = g + ik \tag{2}$$

where g is the damping perturbation introduced in the system. The first step is to substitute Equation (2) into Equation (1) and then put the equation of motion in state-space, like this:

$$\left[\tilde{A} - gI\right]\{\bar{\xi}\} = 0 \tag{3}$$

where:

$$\tilde{A} = \begin{bmatrix} 0 & I \\ -\bar{M}^{-1}\tilde{K} & -\bar{M}^{-1}\tilde{B} \end{bmatrix} \tag{4}$$

$$\bar{M} = \left(\frac{V}{L}\right)^2 M \tag{5}$$

$$\tilde{B} = 2ik\left(\frac{V}{L}\right)^2 M - \frac{1}{2}\rho V^2 Q'(ik) + \left(\frac{V}{L}\right) Z \tag{6}$$

$$\tilde{K} = -k^2\left(\frac{V}{L}\right)^2 M + K - \frac{1}{2}\rho V^2 Q(ik) + ik\left(\frac{V}{L}\right) Z \tag{7}$$

Now, it is necessary to find the roots of this equation of motion in state-space form. For the g-method this is achieved by varying the reduced frequency from zero to a determined maximum value.

The flutter frequency and associated damping is, then determined by:

$$\omega_f = k\left(\frac{V}{L}\right) \tag{8}$$

$$2\gamma = 2\frac{Re(g)}{k} \tag{9}$$

From Equation (8) and Equation (9) is possible to determine the Vgf (velocity and damping versus frequency) curves. These curves contain both damping and frequency evolution for each aeroelastic mode. Also, it is possible to investigate which structural modes couple, that is, the flutter mechanism, and provide solutions to avoid it. All flutter investigation is possible due to these two curves.

2.2 Nonlinear Aeroelastic System

The nonlinear aeroelastic system might be deduced from energy methods. In Aero Flex tool, implemented in MatLab™, the virtual work method and the variation of the energy functional were used. In order to define a tridimensional system, it is decomposed into a transversal section analysis combined with the analysis of a unidimensional beam. All deformations are considered (extension, bending and torsion). With this approach it is possible to calculate aeroelastic systems with big displacements [4].

Consider the following structural dynamics equation [4]:

$$M(\varepsilon)\ddot{\varepsilon} + C(\varepsilon,\dot{\varepsilon})\dot{\varepsilon} + K(\varepsilon)\varepsilon = R \tag{10}$$

where:

$$M(\varepsilon) = J_{h\varepsilon}^T M J_{h\varepsilon} \tag{11}$$

$$C(\varepsilon,\dot{\varepsilon}) = J_{h\varepsilon}^T M \dot{J}_{h\varepsilon} + C \tag{12}$$

$$K(\varepsilon) = K \tag{13}$$

$$R = J_{p\varepsilon}^T F_{pt} + J_{\theta\varepsilon}^T M_{pt} + J_{p\varepsilon}^T B^F F_{dist} + J_{\theta\varepsilon}^T B^M M_{dist} \tag{14}$$

In Equations (11) to (14), M, C and K are structural mass, damping and stiffness, respectively. The Jacobian matrices $J_{h\varepsilon}$, $J_{p\varepsilon}$ and $J_{\theta\varepsilon}$ relate the structural deformations to translation and rotation of each node. They are nonlinear function of the deformation vector ε [4]. R is the total forces and moments acting on the aeroelastic system (pt for punctual or concentrated and $dist$ for distributed). Although Aero Flex has three different ways to calculate the aerodynamic forces and moments acting on the system, only the unsteady was used in this case. So, the lift and the aerodynamic moment are [4]:

$$L = \pi\rho b^2(-\ddot{z} + \dot{y}\dot{\alpha} - ab\ddot{\alpha}) + 2\pi\rho b\dot{y}^2\left[-\frac{\dot{z}}{\dot{y}} + b(0.5-a)\frac{\dot{\alpha}}{\dot{y}} - \frac{\lambda_0}{\dot{y}}\right] \tag{15}$$

$$M_{ea} = Lab + 2\pi\rho b^2\left(-\frac{1}{2}\dot{y}\dot{z} - \frac{1}{2}ab\dot{y}\dot{\alpha} - \frac{1}{2}\dot{y}\lambda_0 - \frac{1}{16}b^2\ddot{\alpha}\right) \tag{16}$$

ρ is the air density, b is the half-chord length, a is position of the aerodynamic center relative to the elastic axis, $\dot{\alpha}$ is the pitch rate, λ_0 is the lag term, y is the axis parallel to the airfoil zero lift line and z is perpendicular upwards. More details on this formulation can be found in Cardoso Ribeiro [4].

2.3 0-1 Test

The system's dynamics reconstruction using Takens' theorem [6], which is the usual method to verify if a system presents chaotic behavior, can lead to some difficulties, especially in determining the embedding dimension and delay parameter, which are fundamental for a reliable result and are not trivial to determine. A poor choice of these parameters leads to wrong attractor, so a wrong dynamic.

A new test for chaos, called 0-1 test, applies directly to the experimental data, so the phase space reconstruction is no longer necessary [5]. Also, it can be applied to all dynamical systems, e.g., continuous or discrete, governed by ordinary or partial differential equations, experimental data, maps, etc [11]. It has presented a great performance when dealing with noisy data and it leads to a binary conclusion (does or does not have chaotic behavior are the only two possible results) [12].

Consider $\phi(j)$ the observed experimental data, for $j = 1,2,\dots,N$. For $c \in (0,\pi)$, where c is chosen randomly, the translation variables are:

$$p_c(n) = \sum_{j=1}^{n} \phi(j) \cos jc \tag{17}$$

$$q_c(n) = \sum_{j=1}^{n} \phi(j) \sin jc \tag{18}$$

The p_c versus q_c plot gives if the system behavior is diffused, like a Brownian movement (chaotic) or bounded (periodic or quasi-periodic). This behavior can be obtained by analyzing the mean square displacement. If it results in a bounded function in time, the dynamics is regular, but if it scales linearly with time, the dynamics is chaotic. The mean square displacement is given by [13].

$$M_c(n) = \lim_{N\to\infty} \frac{1}{N} \sum_{j=1}^{N} \{[p_c(j+n) - p_c(j)]^2 + [q_c(j+n) - q_c(j)]^2\} \tag{19}$$

In practice $n_{cut} = N/10$. The periodic component of the mean square displacement is given by [13]:

$$V_{osc}(c,n) = (E\phi)^2 \frac{1-cos(nc)}{1-cos(c)} \tag{20}$$

where the expectation $E\phi$ is [13]:

$$E\phi = \lim_{N\to\infty} \frac{1}{N} \sum_{j=1}^{N} \phi(j) \tag{21}$$

For better convergence properties, the periodic component is subtracted from mean square displacement, since this result will present the same asymptotic growth as the mean square displacement [13]:

$$D_c(n) = M_c(n) - V_{osc}(c,n) \tag{22}$$

After calculating the Equation 15 up to n_{cut},the asymptotic growth rate is calculated using a correlation method [13]:

$$K_c = corr(\xi, \Delta) = \frac{cov(\xi,\Delta)}{\sqrt{var(\xi)var(\Delta)}} \in [-1,1] \tag{23}$$

ξ is the vector from one up to n_{cut} and Δ is the vector formed by the results from Equation (22). Calculations in Equations (17) to (23) are repeated for a batch of random values of c in the interval $(0, \pi)$. Usually $N_c = 100$ will suffice. The result is obtained from the median of the N_c results of Equation (23) [13]:

$$K = median(K_c) \tag{24}$$

Equation (24) will result in either zero or one. If the result is zero, the system has no chaotic behavior (might be periodic or quasi-periodic). If the result is one, the system presents chaotic behavior. It is important to observe that this test is not to determine if the system presents a stochastics dynamic. This test is applied only to deterministic systems.

This is a very important test, also simple and fast to have a result. Its reliability was questioned once, and the authors proved these questioning to be unfounded [14]. They also presented

mathematical results on the validity of the 0-1 test [15] and the test was applied for a bipolar motor which dynamics could be changed from periodic to chaotic [11].

In this case, the 0-1 test was performed in Matlab™ using the time history for each model modification (slender body center of gravity position).

3 LINEAR FLUTTER PREDICTION

The wing model is an aluminum flat plate with a brass slender body at its tip (Figure 1). This construction allows the center of gravity (CG) to be changed, in order to study this effect in flutter velocity [2].

Figure 1: Wind tunnel model [2].

The computational results, which were obtained from ZAERO® software using g-method, are presented below [2] :

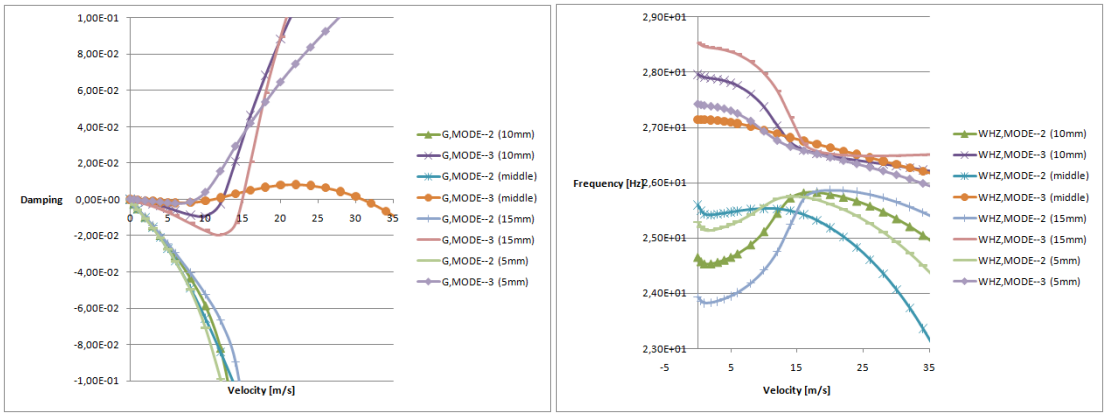

Figure 2: Left: Damping and Right: Frequency versus velocity evolution curves [2].

Figure 2 shows the frequency and damping evolution for each CG position. Since the structure is a flat plate, the elastic center is located at the center (middle chord line). The slender body CG position was varied from 5mm forward the middle until 15mm forward. The flutter velocities and frequencies are presented in Table 3 and compared with experimental results.

For the slender body CG located at the middle chord line, the computational result shows a hump mode (orange curve in Figure 2). However, this mode was not observed during the tests, since the structural damping usually shifts the velocity axis up by an amount given by ground vibration test (GVT), which was not conducted for these models. Then, these linear computational results should be more conservative when compared with the experimental results.

4 NONLINEAR COMPUTATIONAL RESULTS

The AeroFlex Code was used to reproduce the same conditions of the wind tunnel tests. So, not only the model was characterized in the same fashion as the wind tunnel, but also the sampling frequency and time. This was fundamental, so the simulation shall be comparable to the wind tunnel tests. The sampling time considered is 10 seconds with a time step of 0.0002 second.

In order to have a more representative system, the unsteady Peters' model was used to calculate the aerodynamic forces and moments. For the first two cases (slender body CG at 5mm and 10mm), it shall be employed two aerodynamic lag states, which makes the flutter velocities closer to the one measured at the wind tunnel. Meanwhile, for slender body CG 15mm forward mid-chord line, it was necessary to employ four aerodynamic lag states to best represent the system dynamics. These shall be the values applied in the simulations presented next.

4.1 CG 5mm forward mid-chord line

The first simulation result shall be with the slender body CG position located at 5mm forward mid-chord line (or elastic axis). The simulation time is stablished in 15 seconds, so in the 0-1 test evaluation, the 5 seconds transient might be ignored, so the computational experiment time is 10 seconds, like the wind tunnel test. In this manner, both the wind tunnel experiment and the computational experiment have the same test conditions and the comparison between them are in the same base.

The wing tip displacement time history is shown below:

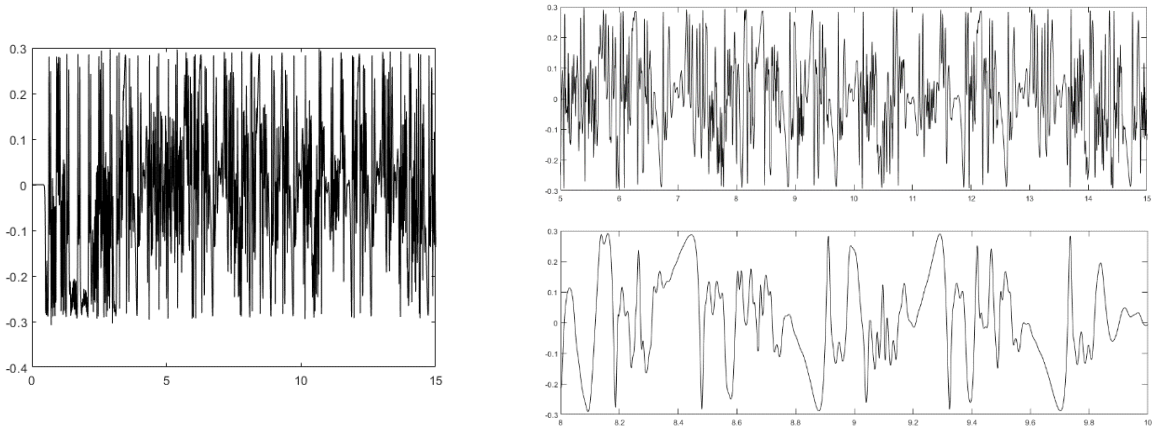

Figure 3: Wing tip displacement time history for CG at 5mm.

In the Figure 3, the graphic in the left-hand side represents the entire time history, including the transient. For analysis purposes and in order to have the same amount of points as the wind tunnel experiment, only 10 seconds shall be considered, so to top right-hand side of the Figure 3 shows the time history that shall be used. The bottom right-hand side of the Figure 3 is an ampliation between 8 seconds and 10 seconds time instants. From this ampliation, it is possible to observe no usual oscillatory, that might be approximated by a simple sine. It looks chaotic.

Like usually is done for any experimental analysis, the FFT and the PSD is calculated from the time history presented in Figure 4:

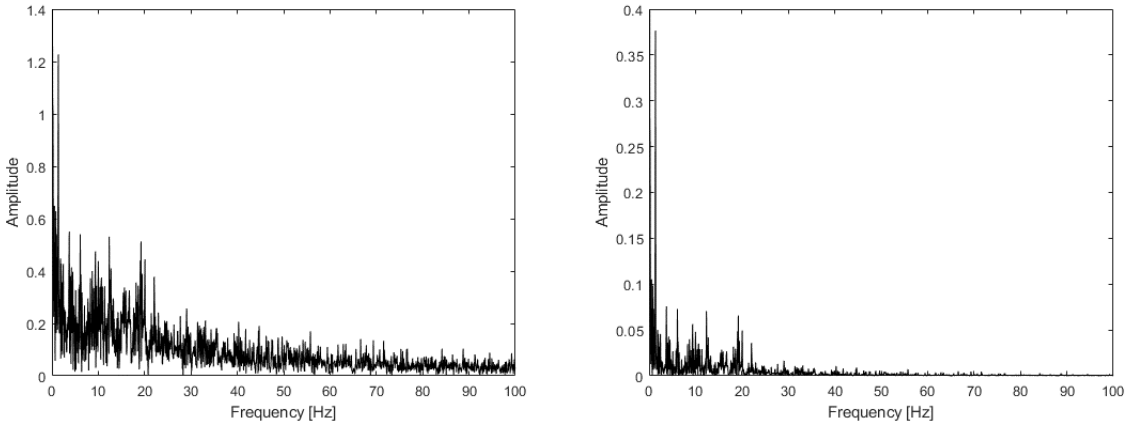

Figure 4: FFT and PSD, respectively, for CG at 5mm.

From Figure 4, there is another indication of chaos: the absence of a prominent peak [16]. It is not possible to determine the flutter frequency by observing the PSD curve. The PSD peaks do not occur only in multiple frequencies, which does not offer any clue about the nonlinear phenomena observed, like saturation phenomenon. The flutter frequency calculated by AeroFlex is 26.7444Hz and the flutter speed is 9.1479m/s.

4.2 CG 10mm forward mid-chord line

The next case is the slender body CG located at 10mm forward the mid-chord line. The same simulation parameters are set as the case before that and as the wind tunnel experiment. The wing tip displacement time history is:

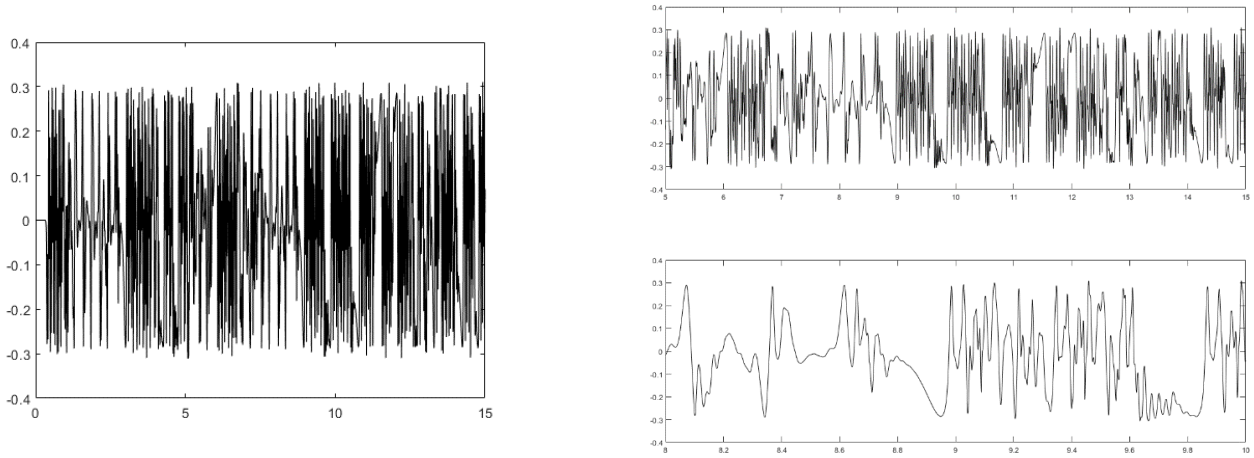

Figure 5: Wing tip displacement time history for CG at 10mm.

The time history in Figure 5, also indicates a chaotic behavior, like the previous case, but more analysis is necessary. The FFT and PSD are:

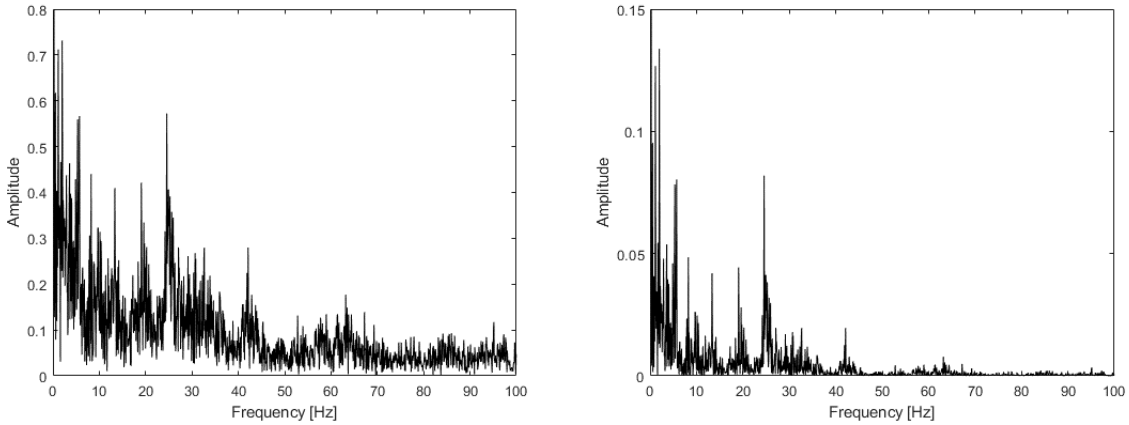

Figure 6: FFT and PSD, respectively, for CG at 10mm.

Again, like in the 5mm CG case, there are multiple peaks, but this time they are in lower amplitude, making it more difficult to distinguish the frequencies that characterize the system dynamics from another signal noise. This means that the system dynamics might present chaotic behavior, like the previous case. The flutter frequency determined by AeroFlex is 26.5327Hz and the flutter speed is 12.7879m/s.

4.3 CG 15mm forward mid-chord line

The simulation time history for slender body CG at 15mm from mid-chord line is:

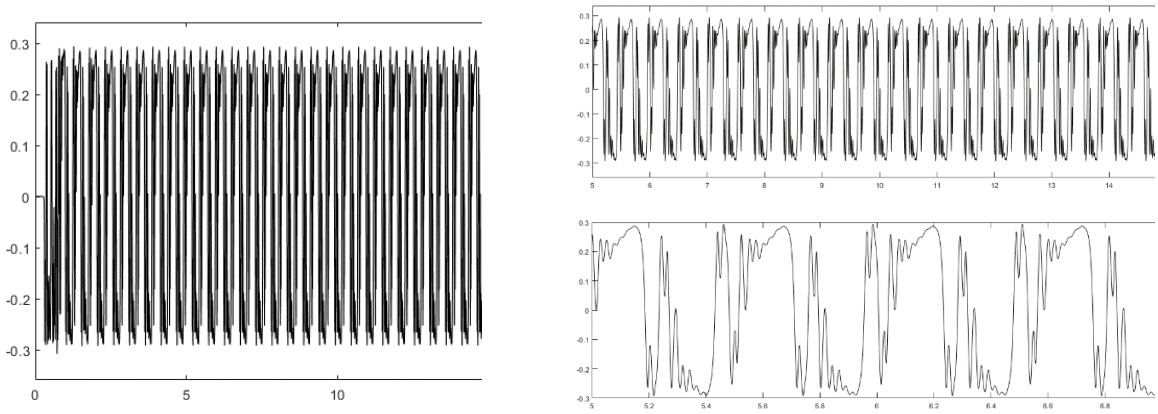

Figure 7: Wing tip displacement time history for CG at 15mm.

Differently from the observed results so far, there is a pattern observed in the wing tip displacement for slender body CG at 15mm it happens every 0.2 second. This oscillatory characteristic shall indicate periodic dynamics. The FFT and PSD are:

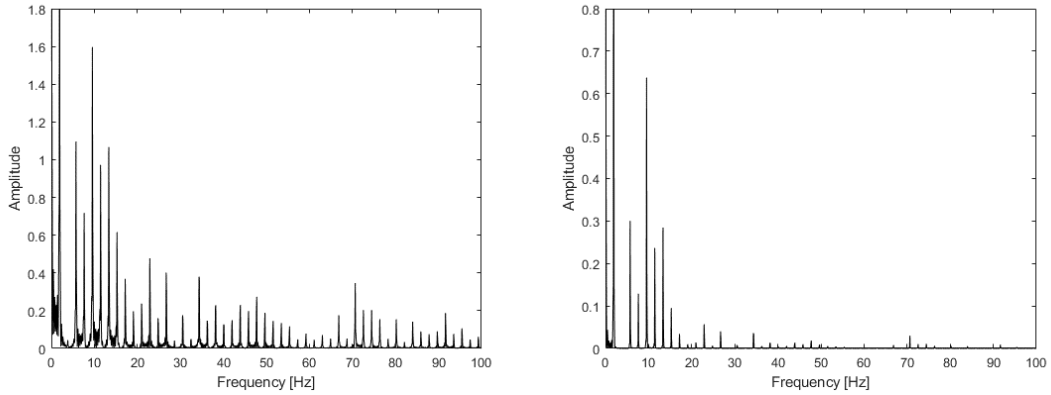

Figure 8: FFT and PSD, respectively, for CG at 15mm.

In this case there are multiple well-defined frequencies peaks. The flutter frequency calculated by AeroFlex is 26.3704Hz and the flutter speed is 14.6880m/s. This system is dominant by another frequency, different from flutter frequency. It is expected to obtain a periodic behavior result in 0-1 test for chaos.

It is important to highlight that the experiment measurements were at the wing root, not the wing tip, different from the simulations presented in this chapter. All differences observed here, might be firstly attributed by this factor. The experiments might be conducted again following the same set up of the simulations, since it has less signal noise the wing tip displacement, instead of root acceleration.

5 EXPERIMENTAL RESULTS

All the tests results presented in this chapter are from wind tunnel flutter tests [2]. They were validated using commercial software: NASTRAN® to obtain the modal basis and ZAERO® (g-method) to obtain the flutter velocity and frequency, as well as the aeroelastic modes evolution. The g-method equations are presented in section 2. Nevertheless, for more details about flutter theoretical background and these tests, the reference [3] shall be consulted.

The experimental procedure for this test was:

1) The model is clamped at the support shown in Figure 9;

2) The wind tunnel is turned on and the velocity is slowly increased as the PSD is monitored on the laptop;

3) As the model starts to vibrate, the PSD (power spectral density) curve presents a sharp peak. This is the moment which flutter is observed. The PSD approach was employed as one way to identify flutter [2]. The output signal from an accelerometer, through its PSD computation, identifies the flutter onset condition and the corresponding undisturbed flow speed. The sharp peak represents the flow's energy that the model extract to flutter.

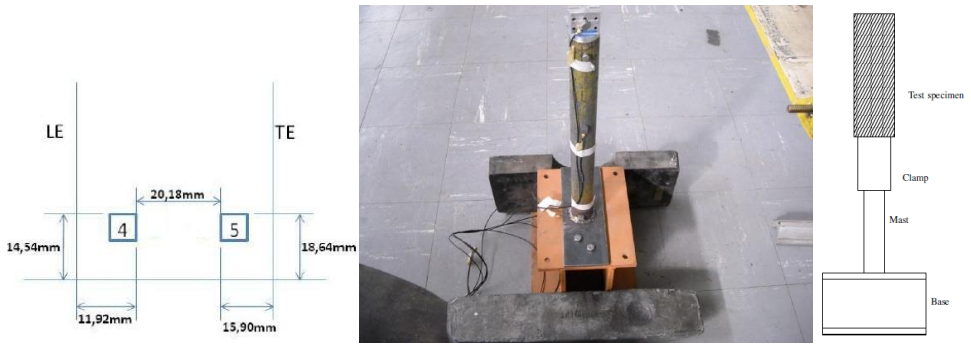

Figure 9: Support model [9].

4) The slender body CG is changed and steps 2 and 3 are repeated.

5) The acceleration time history is recorded for 10 seconds for each experiment. These results are presented here (Figure 10:, Figure 12: Time histories for CG at 10mm [9].

, **Erro! Fonte de referência não encontrada.**). The left-hand side of Figure 10 shows the accelerometers positioning. They were located at the wing root.

Since the model did not fail as expected by linear theory, this system might present some nonlinearity. Aeroelastic systems may present structural or aerodynamic nonlinearities. The aerodynamic nonlinearities are related to shock waves in transonic flow, dynamic stall or wing tip vortices [17]. For the aeroelastic system presented, only the first (shock waves) are impossible to happen, since the flow in this test was in low subsonic. Dynamic stall has been reported in helicopter blades even in low velocity. And wing tip vortices might oscillate with the wing model [17]. However, since this model present high aspect ratio and high flexibility, the structural nonlinearity seems to be more likely to dominate over the aerodynamic effects [18].

5.1 CG 5mm forward mid-chord line

The acceleration time history and the integrated signal to obtain velocity and displacement are shown below:

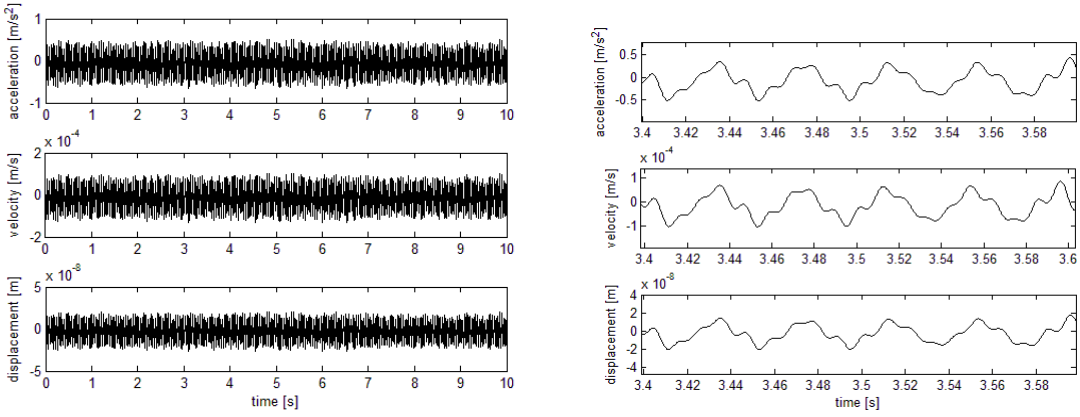

Figure 10: Time histories for CG at 5mm [9].

Figure 10 shows the accelerometer time history and both integrated signals for velocity and displacement. The figure at the right shows only between 3.4 and 3.6 seconds acquisition, while at the left shows the entire acquired data. This data was recorded after the flutter phenomena was observed. The FFT and PSD are:

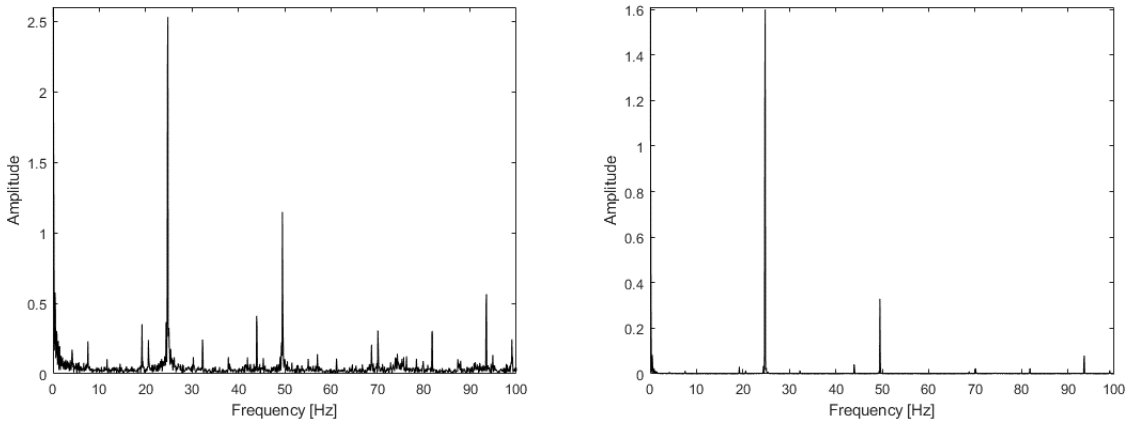

Figure 11: Left: FFT and right: PSD curves for CG at 5mm [9].

From Figure 11, one observes one prominent PSD peak, which is the flutter frequency (24.8Hz). However, there are other smaller peaks. Those frequencies might be analyzed to find nonlinearities due to internal resonances [16]. The internal resonance presence leads to a complete transfer of the energy from the lower frequency mode to the higher frequency mode. This phenomenon is known as saturation and it is a quadratic nonlinearity. The quadratic nonlinearity can be observed as a peak in 49.51Hz. Also, this kind of motion is unstable and leads to amplitude and/or phase modulation.

5.2 CG 10mm forward mid-chord line

The same analysis was proceeded: the system reach flutter and then the data is recorded. The time histories are shown below:

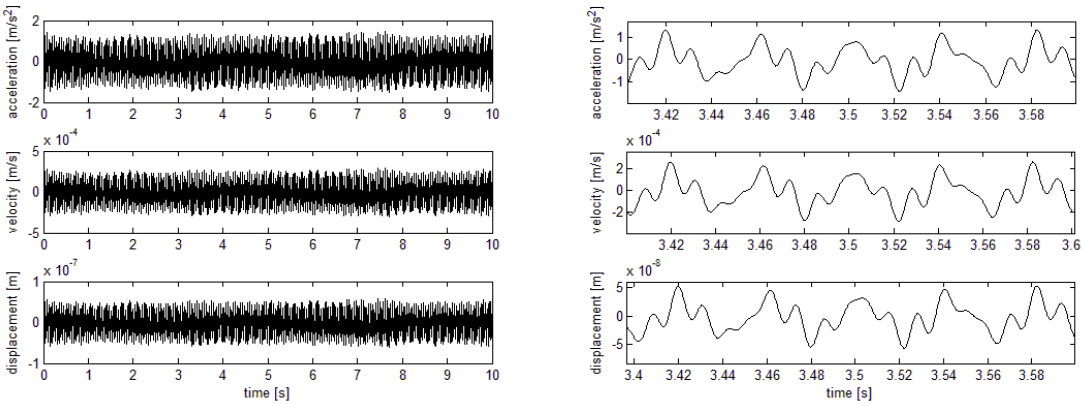

Figure 12: Time histories for CG at 10mm [9].

This is also an accelerometer signal integrated for both velocity and displacement. The Figure in the right hand is the same data, but for 3.4 until 3.6 seconds in order to better visualize and it is possible to observe some periodicity in the signal. The FFT and PSD are calculated:

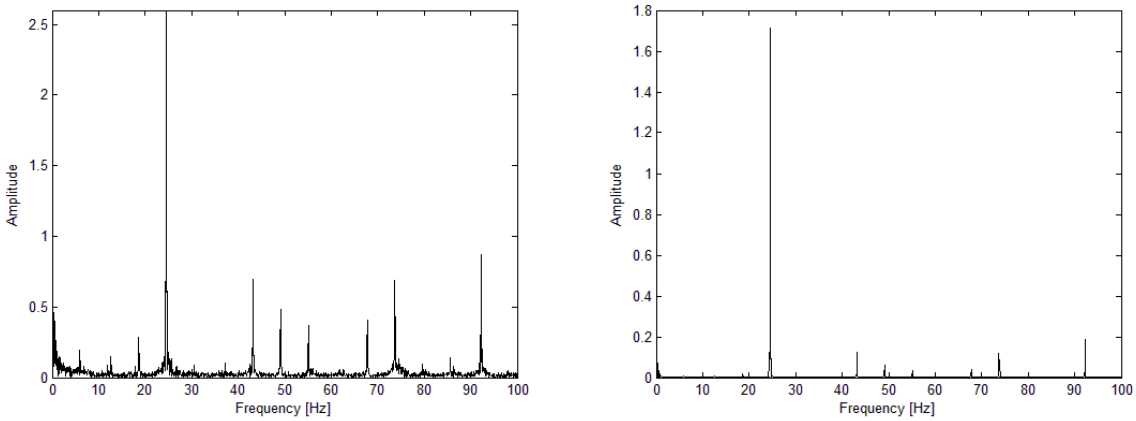

Figure 13: Left: FFT and right: PSD curves for CG at 10mm [9].

From Figure 13, one can observe that the flutter frequency is 24.57Hz. As explained before, the quadratic resonance is due to saturation phenomenon. According to [16], the cubic resonance occurs when the structure presents high flexibility effects. From this analysis, one can conclude that this system is clearly nonlinear and possibly chaotic.

Table 1: Internal and combination resonances.

$\omega[Hz]$	
24.57	Flutter frequency (ω)
49.13	$2 \times \omega$
73.70	$3 \times \omega$

5.3 CG 15mm forward mid-chord line

In the next Figure, the CG is moved another 5mm and the accelerometer time histories and the integrated signal for velocity and displacement are [9]:

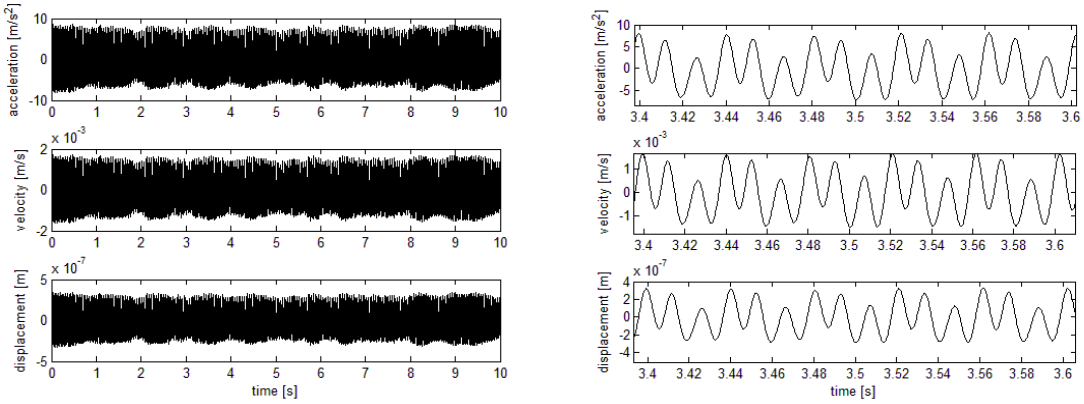

Figure 14: Time histories for CG at 15mm [9].

From the time histories, one has a first clue that this system is periodic. Nevertheless, further analyses are necessary. The FFT and the PSD were also calculated in order to verify the model nonlinearities:

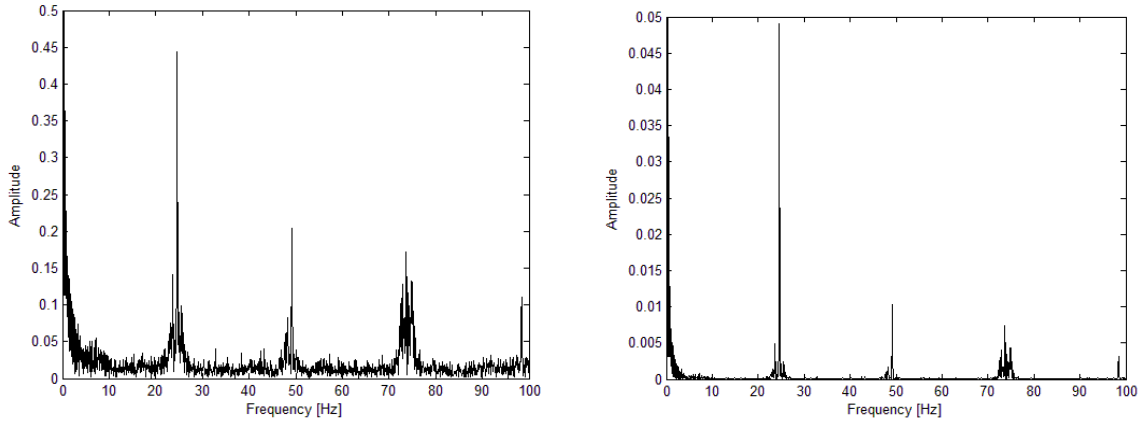

Figure 14: Left: FFT and right: PSD curves for CG at 15mm [9].

In this case, all peaks are flutter frequency multiples. This could be better understood from the next table with the internal and combination resonances. Also, the FFT plot shows clearly defined peaks, with their amplitudes decaying from flutter frequency (the highest). Chaotic systems, in general, have more peaks. So, the PSD plot is important to visualize:

Table 2: Internal and combination resonances.

$\omega[Hz]$	
24.57	Flutter frequency (ω)
49.21	$2 \times \omega$
73.70	$3 \times \omega$
98.42	$4 \times \omega$

From Table 2, this system is complex enough to present quadratic, cubic and fourth order (multiple of quadratic) nonlinearities and according to [16] more than one resonance may occur simultaneously for these cases. All resonance peaks observed in FFT participate in system's dynamics and are multiples of flutter frequency.

The flutter velocity and frequency for each CG case and analysis strategy are presented and compared in Table 3 bellow.

Table 3: Flutter results for each CG position

	Computational Linear	***Computational Nonlinear***	***Experimental***
	CG at 5mm		
Velocity[m/s]	8.1	9.15	9.45
Frequency[Hz]	27.2	26.7	24.7
	CG at 10mm		
Velocity[m/s]	12.3	12.8	12.1
Frequency[Hz]	27.4	26.5	24.6
	CG at 15mm		
Velocity[m/s]	14.6	14.7	14.5
Frequency[Hz]	27.1	26.4	24.7

As it is observed from Table 3, the computational result obtained with ZAERO® and Aero Flex predicted very well the flutter velocity and flutter frequency, comparing to wind tunnel test. This means that the linear theory predicts flutter precisely in a small disturbance context. However, the linear model do not predict if the model will fail or only oscillate after achieving the flutter velocity, which is well predicted by Aero Flex tool.

6 0-1 TEST FOR CHAOS

After these observations from traditional signal analysis, the 0-1 test shall be performed. For CG at 5mm forward the center chord line, the phase portrait of the translation variables p and q, which were already defined in the section 2, are shown in Figure 15. It is a good practice to verify this phase portrait in order to confirm if it represents a Brownian or a bounded movement. This representation is also called auxiliary trajectory [19]:

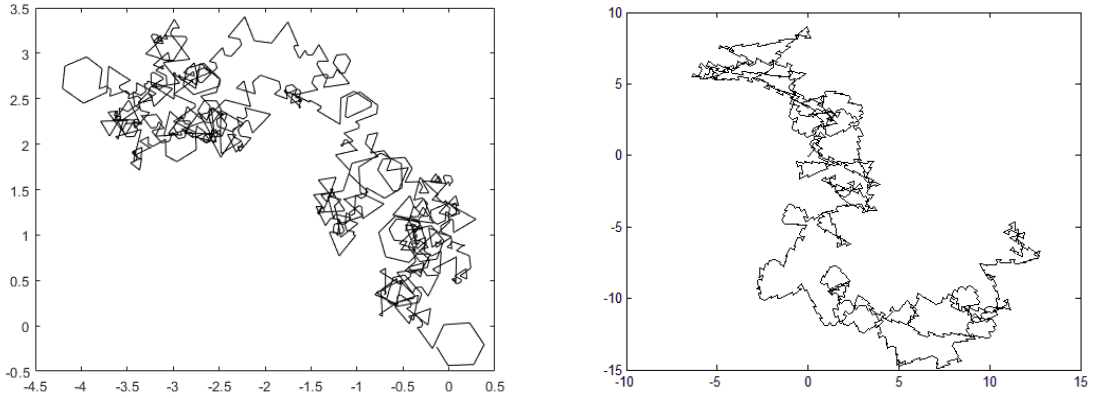

Figure 15: Auxiliary trajectory for CG at 5mm. Left: Computational. Right: Experimental.

The 0-1 test result is 0.9969, for computational analysis using Aero Flex, which indicates that this system presents chaotic behavior. For the experimental time history, the 0-1 test for chaos is conducted and the result for this case is 0.9828, which also indicates that this system presents chaotic behavior. As observed in Figure 15, they both represent Brownian motions (does not have a closed, defined form).

For CG at 10mm, the 0-1 test for both nonlinear computational and experimental results are:

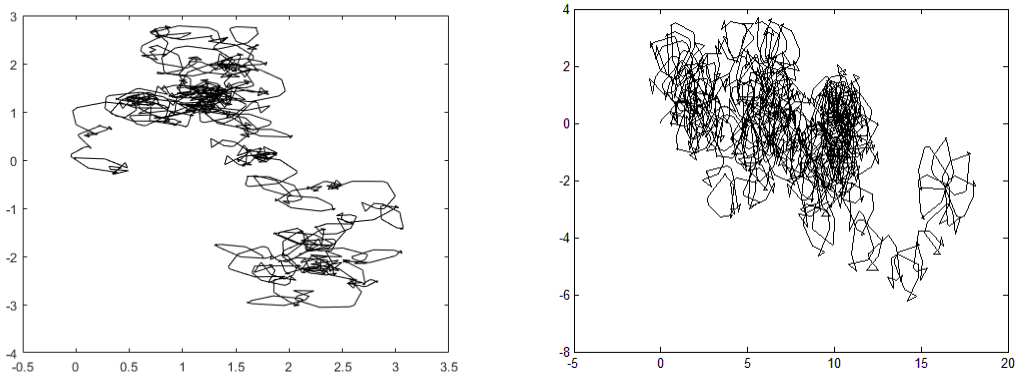

Figure 16: Auxiliary trajectory for CG at 10mm. Left: Computational. Right: Experimental.

Figure 16 shows again Brownian motions. The result of the 0-1 test is 0.9960, which indicates chaotic behavior for the computational time history and 0.9799 for the experimental time history, which also indicates chaotic behavior.

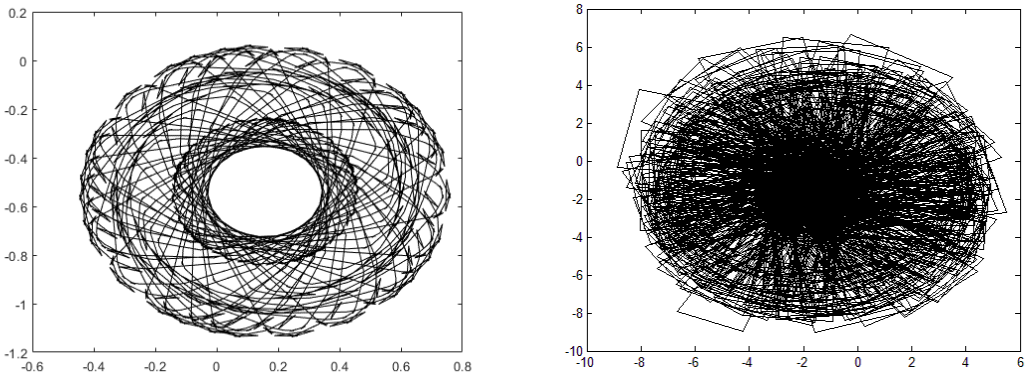

Figure 17: Auxiliary trajectory for CG at 15mm. Left: Computational. Right: Experimental.

Like expected, the auxiliary trajectory result is a well-defined figure, very similar from the figures obtained by [19]. The 0-1 test result is 0.1471, which is not very close from zero, but still can be categorized as periodic behavior [19], in the case of nonlinear computational result. For experimental time history, the 0-1 test for chaos is -5.1993×10^{-4}, which represents a periodic or quasi-periodic dynamic for this specific CG position.

7 CONCLUSIONS

The 0-1 test is a quick, easy and very reliable test for noisy data, which is expected from any experimental result. Since the 0-1 test is easy to implement and has low computational cost (for 50000 data points it took a few seconds in a common laptop), it is recommended its application to all nonlinear aeroelastic tests. Also, one should always perform the oversampling test. The 0-1 test should not be performed for oversampling data in order to avoid mathematical issues.

For this wing model, the system dynamics for CG 5mm and 10mm forward center line were concluded as chaotic only using the 0-1 test. For CG 15mm forward the center line the system dynamics is periodic or quasi-periodic. Also, it is important to build the bifurcation diagram, which might help to understand the system dynamics behavior with the variation of certain parameters, which shall be presented in the future.

As a future work, besides the determination of the bifurcation diagram for these cases, the attractor reconstruction using Takens' theory shall be performed in order to compare the results. Also, different parameters shall be investigated, such as variation in angle of attack, or wing material, by using a composite wing model. The influence of the instrumentation position shall be evaluated, since the PSD curves are different from the obtained using the computation experiment.

8 REFERENCES

[1] Dowell, E. H.; Tang, D. Experimental and Theoretical Study of Gust Response for High-Aspect-Ratio Wing. *AIAA Journal*, vol. 40, p. 419-429, 2002.

[2] Sheta, E. F.; Harrand, V. J.; Thompson, D. E.; Strganac, T. W. Computational and Experimental Investigation of Limit Cycle Oscillations of Nonlinear Aeroelastic Systems. *AIAA Journal*, p. 133-141, 2002.

[3] Westin, M. F. Aeroelastic Modeling e Experimental Analysis of a Flexible Wing for Wind Tunnel Flutter Test. 2010. 92f. Thesis (Master in Aeronautical and Mechanical Engineering) – Aeronautical Institute of Technology, São José dos Campos.

[4] Cardoso Ribeiro, Flávio Luiz. *Dinâmica de Voo de Aeronaves Muito Flexíveis*. 2011. 157f. Tese de Mestrado – Instituto Tecnológico de Aeronáutica, São José dos Campos.

[5] Gottwald, G. A.; Melbourne, I. A New Test for Chaos in Deterministic Systems. *Proceedings of the Royal Society of London A: Mathematical, Physical and Engineering Sciences*, vol. 460, p. 603-611, 2004.

[6] Takens, F. Detecting Strange Attractors in Turbulence, in Dynamical Systems and Turbulence, *Lectures Notes in Mathematics*, vol. 898, p. 366-381, 1981.

[7] Cao, L. Practical method for determining the minimum embedding dimension of a scalar time series, *Phisica D*, v.110, p.43, 1997.

[8] Fraser, A. M.; Swinney, H. L. Independent Coordinates for Strange Attractors from Mutual Information. *Physical Review A*, v.33, pp.1134-1140, 1986.

[9] Westin, M. F.; Silva, R. G. A.; Balthazar, J. M.; Nabarrete, A.; Tusset, A. M.; Ladeira, G. On Nonlinear Wind Tunnel Aeroelastic Tests and Application of 0-1 Test for Chaos. In: 24th ABCM International Congress of Mechanical Engineering, 2017, Curitiba. *Proceedings of the 24th ABCM International Congress of Mechanical Engineering*. COBEM-2017-0201.

[10] Bisplinghoff, R. L. and Ashley, H. *Aeroelasticity*. Addison Wesley, 1955.

[11] Falconer, I., Gottwald, G.A., Melbourne, I. and Wormnes, K. "Application of the 0-1 Test for Chaos to Experimental Data". *SIAM Journal on Applied Dynamical System*, Vol. 6, Issue 2, p. 395-402, 2007.

[12] Gottwald, G.A. and Melbourne, I. "Testing for Chaos in Deterministic Systems with Noise", *Physica D: Nonlinear Phenomena*, Vol. 212, No. 1, p. 100-1120, 2005.

[13] Gottwald, G.A. and Melbourne, I. "On the Implementation of the 0-1 Test for Chaos", *SIAM Journal on Applied Dynamical Systems*, Vol. 8, Issue 1, p. 129-145, 2009.

[14] Gottwald, G.A. and Melbourne, I. "Comment on "Reliability of the 0-1 Test for Chaos"", *Physical Review E*, Vol. 77, No. 2, p. 028201, 2008.

[15] Gottwald, G.A. and Melbourne, I. "On the Validity of the 0-1 Test for Chaos", Nonlinearity, Vol. 22, No. 6, p. 1367, 2009.

[16] Nayfeh, A. H. and Balachandran, B. "Applied Nonlinear Dynamics: Analytical, Computational and Experimental Methods". Wiley VCH, 2004.

[17] Lee, B.H.K, Price, S.J. and Wong, Y.S. "Nonlinear Aeroelastic Analysis of Airfoils: Bifurcation and Chaos". Progress in Aerospace Sciences, Vol.35, p. 205-334, 1999.

[18] Dowell, E., Edwards, J. and Strganac, T. "Nonlinear Aeroelasticity". Journal of Aircraft, Vol. 40, September-October, 2003, p. 857-874.

[19] Bernardini, D.; Litak, G. An Overview of 0-1 Test for Chaos. *Journal of the Brazilian Society of Mechanical Sciences and Engineering*, vol. 38, p. 1433-1450, 2016.

COPYRIGHT STATEMENT